Study of the Glass Transition Temperature of Polymer Surface by Coarse-Grained Molecular Dynamics Simulation

Hiroshi Morita,*,† Keiji Tanaka,‡ Tisato Kajiyama,§ Toshio Nishi,⊥ and Masao Doi†

Japan Science and Technology Agency & Department of Applied Physics, The University of Tokyo, 7-3-1 Hongo, Bunkyo-ku, Tokyo 113-8656, Japan; Department of Applied Chemistry, Kyusyu University, 744 Motooka, Nishi-ku, Fukuoka 819-0395, Japan; Kyusyu University, 6-10-1 Hakozaki, Higashi-ku, Fukuoka 812−8581, Japan; and Department of Organic and Polymeric Materials, Tokyo Institute of Technology, 2-12-1, Ohokayama, Meguro-ku, Tokyo 152-8552, Japan

Received December 9, 2005; Revised Manuscript Received May 8, 2006

ABSTRACT: The glass transition temperature at the surface of polymer film is studied by the coarse-grained molecular dynamics simulation. By the analysis of the segmental motion, the glass transition temperatures at the surface region and that in the bulk region are determined separately. The glass transition at the surface region is found to be lower than that in the bulk region. The molecular weight dependence of the glass transition temperature obtained by the simulation agrees well with that obtained by the scanning force microscopic measurements.

1. Introduction

The glass transition of polymer film is an important problem in many microprocesses of polymers such as coating and printing.[1] Experimental studies[1−12] indicate that the glass transition temperature T_g of ultrathin polymer films is different from that of the bulk, and depends on the film thickness: T_g increases or decreases depending on the interaction between the film and the materials sandwiching the film (the air or the base substrate). This change in T_g has been considered to be caused by the interaction between the polymer phase and the outer phase. Kajiyama et al.[2−4] confirmed this directly. They measured the friction force of a probe tip on the polymer surface as a function of the temperature and showed that it changes drastically at a certain temperature which they called the surface glass transition temperature (T_g^s). They showed that T_g^s is considerably (40−80 K) lower than that in the bulk.

In the previous paper,[13] we have shown that the result of the frictional force measurement of a probe tip done by Kajiyama et al. can be reproduced by molecular dynamics simulation. However, the comparison was limited to qualitative aspects. In this paper, we will make quantitative comparison with the experiment.

Many molecular dynamics studies have been done for the glass transition of the film of polymer melts[14−17] or grafted polymer.[17,18] Most of the previous studies were focused on the problem of how the glass transition temperature depends on the film thickness. Few studies have been done for the problem how the glass transition at the surface differs from that in the bulk. An exception is the recent work of Yoshimoto et al.[19] They calculated the dynamic modulus of polymer film as a function of the distance from the surface and discussed the glass transition temperature.

In this paper, we shall use a simple method to determine T_g. We shall calculate the mean-square displacement of polymer segment (in a certain fixed time interval) as a function of the temperature and determine T_g from the plot. Although it is simple, the method gives a good agreement for T_g with that obtained from the analysis of the free volume in the bulk. It also gives a good agreement with that obtained by scanning force microscopy.

2. Simulation Method

2.1. Polymer. We used the bead−spring model of Grest and Kremer.[20] The polymer consists of N beads connected by the following potential $U^B(r)$

$$U^B(r) = U^{FENE}(r) + U^{LJ}(r) \tag{1}$$

where r is the distance between the beads. $U^{FENE}(r)$ and $U^{LJ}(r)$ are given by

$$U^{FENE}(r) = \begin{cases} -\frac{1}{2} kR_0^2 \ln\left(1 - \left(\frac{r}{R_0}\right)^2\right), & (r \le R_0) \\ \infty, & (r > R_0) \end{cases} \tag{2}$$

$$U^{LJ}(r) = \begin{cases} 4\epsilon\left[\left\{\left(\frac{\sigma}{r}\right)^{12} - \left(\frac{\sigma}{r}\right)^{6}\right\} - \left\{\left(\frac{\sigma}{r^{cut}}\right)^{12} - \left(\frac{\sigma}{r^{cut}}\right)^{6}\right\}\right], & (r \le r^{cut}) \\ 0, & (r > r^{cut}) \end{cases} \tag{3}$$

where k is the spring constant, R_0 is the maximum extension of the spring, ϵ is the unit of the energy, and σ is the unit of length. The nonbonding interaction between the polymer segments separated with the distance r is also given by the Lennard-Jones potential $U^{LJ}(r)$.

The time evolution of beads at position $\mathbf{r}_n$ is calculated by the Langevin equation

$$m\frac{d^2\mathbf{r}_n}{dt^2} = -\frac{\partial U}{\partial \mathbf{r}_n} - \Gamma\frac{d\mathbf{r}_n}{dt} + \mathbf{W}_n(t) \tag{4}$$

where m is the mass of beads, U is the total potential energy of the system, Γ is the friction constant, and $\mathbf{W}_n(t)$ is a Gaussian white noise which is generated according to the following equation:

$$\langle \mathbf{W}_n(t)\, \mathbf{W}_m(t')\rangle = 2k_B T m\Gamma\delta_{nm}\mathrm{I}\delta(t - t') \tag{5}$$

† The University of Tokyo.
‡ Department of Applied Chemistry, Kyusyu University.
§ Kyusyu University.
⊥ Tokyo Institute of Technology.
* Corresponding author: Tel and Fax +81-3-5841-6833; e-mail hmorita@rheo.t.u-tokyo.ac.jp.

10.1021/ma052632h CCC: $33.50
Published on Web 08/02/2006

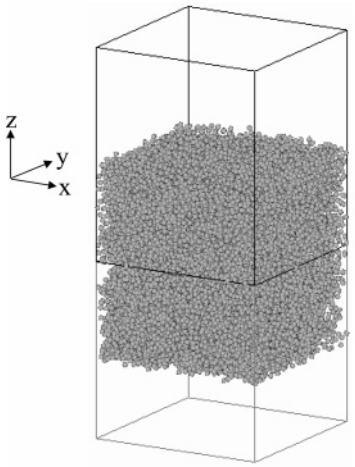

Figure 1. Model of polymer film used in the present work. The system consists of 100 chains each consisting of 100 beads. The size of the simulation box is $32\sigma \times 32\sigma \times 32\sigma$.

We used the following parameter set: $k = 30.0\epsilon/\sigma^2$, $R_0 = 3.0\sigma$, $r^{cut} = 2.0\sigma$, and $\Gamma = 0.5\tau^{-1}$, where τ is the unit of time given by $\sigma(m/\epsilon)^{1/2}$. These parameters are the same as that of Grest and Kremer except for r^{cut}. The interval of one time step is 0.01τ. The unit of temperature is $T_0 = k_B/\epsilon$.

2.2. Polymer Film. We consider a free-standing polymer film placed normal to the z axis (see Figure 1) extending infinitely in x and y directions. We conducted the simulation in a box of size $L \times L \times L$. We used the periodic boundary condition for the boundary normal to the x and y axes; i.e., if a bead exists at (x, y, z), image beads are assumed to exist at $(x \pm L, y \pm L, z)$. For the boundary at $z = 0$, we used the staggered reflective boundary condition;[21] i.e., image beads are assumed to exist at $(x \pm L/2, y \pm L/2, -z)$.

In conducting the simulation, we first constructed the equilibrium polymer configuration at high temperature ($T = 1.0T_0$) using the density-biased Monte Carlo method (DBMC) proposed by Aoyagi et al.[21] In this method, the probability of finding nth segment at position z is calculated by solving the one-dimensional self-consistent-field equation,[18,21] and the polymer chains are generated using this probability. Starting from the system, we obtained the equilibrium configuration by computational annealing, i.e., conducting the MD calculation at fixed temperature for an extended period of time. Polymer configuration at lower temperature was obtained by decreasing the temperature and equilibrating the system.

All simulation was done for fixed number of beads of 10 000. The number of chains was varied when the molecular weight N (i.e., the number of beads per chain) is changed. The simulation was done in the box of fixed size $32\sigma \times 32\sigma \times 32\sigma$. When the temperature was changed, we performed the simulation for 1 500 000 time steps to relax the system and then continued the simulation for another 1 500 000 time steps to get the data for analysis.

Figure 1 shows an example of the configuration for the simulation. The figure shows twice of the actual simulation box since the staggered reflective boundary condition is used: the chain in the bottom box is a mirror image of that in the top box with half-periodicity shifted. The thickness of the film is about 30σ, which is sufficiently larger than the root-mean-square of the polymer in the bulk region even for the largest polymer of $N = 200$.

Figure 2 shows the density distribution across the film for the polymer of $N = 100$. The figure indicates that the width of the surface region is about $3-4\sigma$. layers. This value agrees reasonably well with the previous works.[17,19] Notice that the density is flat near $z = 0$, indicating that the staggered reflective boundary condition is a natural boundary condition for the bulk.

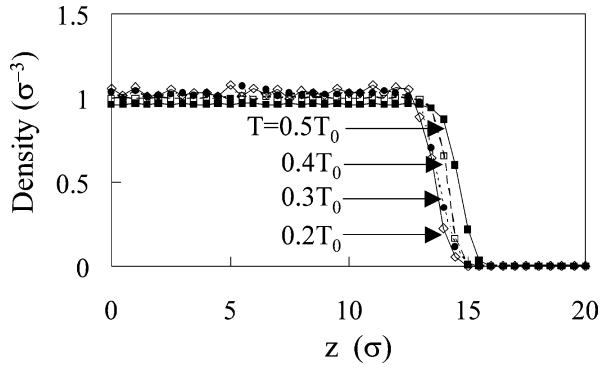

Figure 2. Density profile across the film is plotted for various temperatures. The vertical axis stands for the density averaged over the layer of thickness 0.5σ.

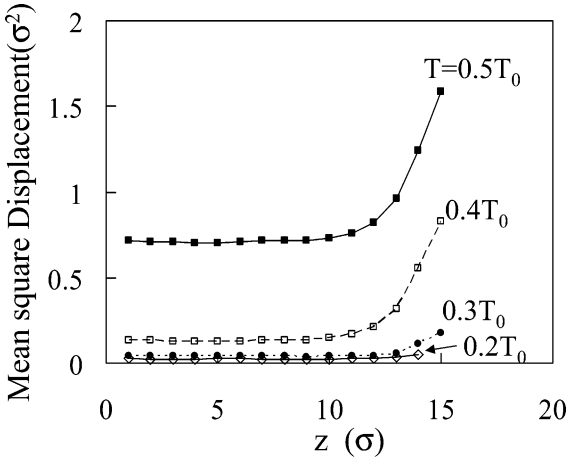

Figure 3. Mean-square displacement of a polymer segment in a time interval t^* is plotted against the mean z position of the segment for various temperatures ($N = 100$). The average is taken for each layer of thickness 1σ.

3. Results and Discussion

3.1. Analysis of Segment Motion at the Surface. To study the segment mobility near the surface, we divided the film into layers normal to the z axis and calculated the mean-square displacement of the segment in each layer in a time interval t. The thickness of the layer is σ, and a segment n is regarded to be in the layer ℓ for the time interval between t' and $t' + t$ if the average z coordinate $[z_n(t') + z_n(t' + t)]/2$ is between $\sigma\ell$ and $\sigma(\ell + 1)$. The mean-square displacement of the segment in the layer ℓ is defined by

$$\phi_\ell(t) = \frac{\sum_{t'} \sum_{n \text{ in layer } \ell} [r_n(t' + t) - r_n(t')]^2}{\sum_{t'} \sum_{n \text{ in layer } \ell} 1}. \qquad (6)$$

It must be mentioned that $\phi_\ell(t)$ become inappropriate to characterize the surface mobility if t is taken to be very large: for large t, the diffusion of segments blurs the layer dependence of $\phi_\ell(t)$. For small t, however, $\phi_\ell(t)$ is a convenient to quantity to characterize the surface mobility. In the following we will choose a specific time $t^* = 50\tau$: the reason for this choice will be discussed later.

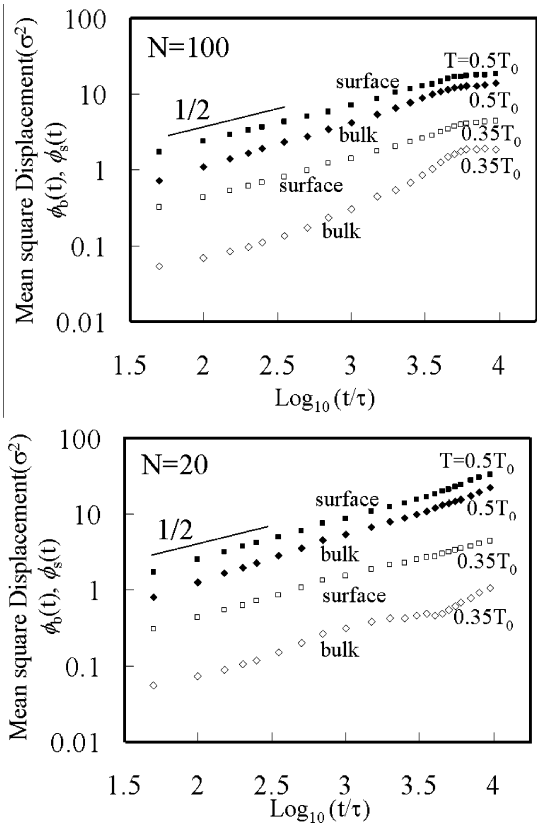

Figure 4. Mean-square displacement of a polymer segment in the bulk region ($\phi_b(t)$) and that in the surface region ($\phi_s(t)$) are plotted against time t: (top) result of the chain of $N = 100$; (bottom) that of $N = 20$. Temperatures are indicated in the figure.

Figure 3 shows $\phi_l(t^*)$ as a function of $z = \sigma/$ for various temperatures. It is seen that the segmental mobility near the surface differs significantly from that in the inner region and that this surface region is limited to the thickness of about 3σ, which is about the same as that determined by the density profile. In the following, we will analyze the segment mobility for the first three layers near the surface separately from that in the bulk region.

Figure 4 shows the mean-square displacement of segment in the entire time region ($t = 50\tau$ to 10000τ) at various temperature and chain length. Here the mean-square displacement of the surface $\phi_s(t)$ is the average of $\phi_l(t)$ for the three layers near the surface, and that for the bulk $\phi_b(t)$ is the average for the three layers near the center.

It is seen that $\phi_s(t)$ is larger than $\phi_b(t)$ in the entire time region, indicating that the segmental mobility near the surface is higher than that in the bulk and that both functions have the scaling form

$$\phi_s(t) = \sigma^2\left(\frac{t}{\tau_s}\right)^{\alpha} \qquad \phi_b(t) = \sigma^2\left(\frac{t}{\tau_b}\right)^{\alpha} \tag{7}$$

for the time region $t < 3000\tau$, where τ_s and τ_b are the times characterizing the local segment in the surface and the bulk region. The exponent α is about 1/2 for both the bulk and the surface region. According to the tube model, this corresponds to the unconstrained Rouse-like motion within a tube.[25]

The temperature dependence of the segmental mobility should, in principle, be characterized by the temperature dependence of τ_s and τ_b. However, since $\phi_s(t)$and $\phi_b(t)$ have the scaling form near $t^* = 50\tau$, we used $\phi_s(t^*;T) = \sigma^2(t^*/\tau_s(T))^{\alpha}$ to characterize the temperature dependence of the segmental mobility. As far as the scaling relation holds, the result is independent of the choice of t^*.

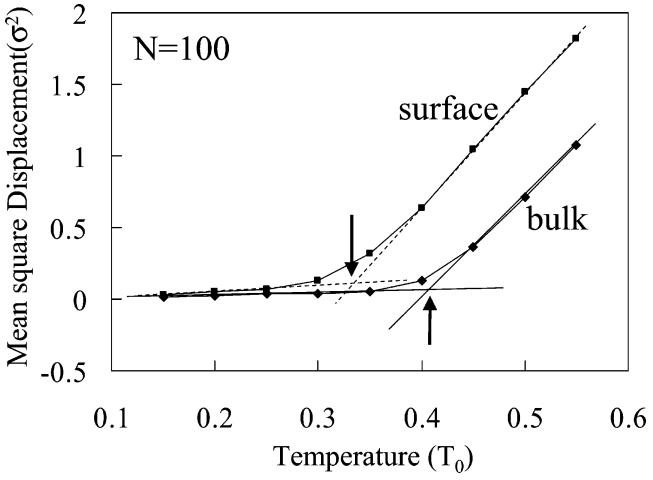

Figure 5. Mean-square displacement of a polymer segment in the bulk region and that in the surface region are plotted against temperature. The arrows indicate the glass transition temperature determined by the present method.

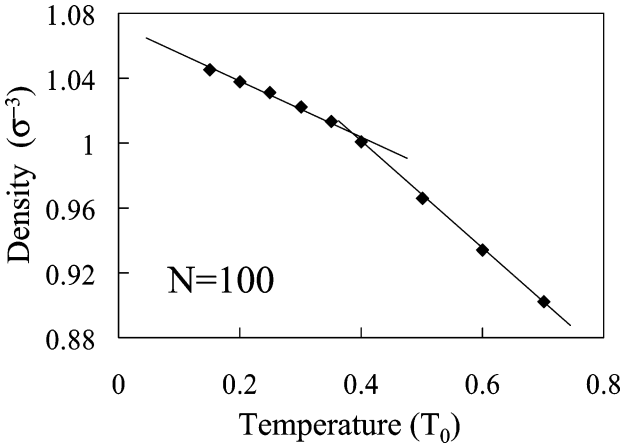

Figure 6. Segment density of the bulk polymer obtained by the MD simulation of constant pressure ($P = 0$) is plotted as a function of temperature.

3.2. Determination of the Glass Transition Temperature. Figure 5 shows the mean-square displacement at the surface ($\phi_s(t^*;T)$) and that in the bulk ($\phi_b(t^*;T)$) plotted against temperature for the chain of $N = 100$. It is seen that the mean-square displacement starts to increase sharply at certain temperature which can be associated with the glass transition temperature. The characteristic temperature can be obtained by the intersection of the two lines characterizing the behavior at low and high temperatures.

To check whether the temperature obtained by this method corresponds to the glass transition temperature obtained by the conventional method, we performed a series of simulation for bulk system using the periodic boundary condition for all the walls and the constant-pressure condition of Andersen,[26] where the pressure is chosen to be zero. We calculated the density as a function of temperature, and the result is shown in Figure 6.

The density has a break point at $T = 0.4T_0$, indicating the glass transition. This temperature is in good agreement with the bulk glass transition temperature shown in Figure 5. This validates the procedure of determining the glass transition temperature of the polymer film in the bulk and the surface region. The surface T_g is lower than the bulk T_g. This result is similar to the experimental results of Tanaka et al.[2]

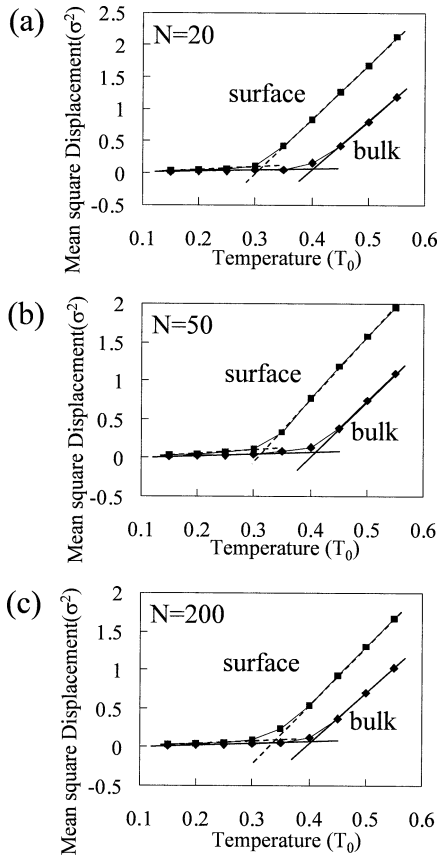

Figure 7. Mean-square displacements of a polymer segment are plotted against the temperature for the case of $N = 20$ (a), 50 (b), and 200 (c).

3.3. Comparison with Experiments. Figure 7 shows the temperature dependence of the mean-square displacement at the surface and in the bulk region for the chain of $N = 20$, 50, and 200. In all cases, the transition temperatures are obtained clearly.

To compare the T_g obtained by the simulation with the experimental T_g of Tanaka et al.,[2] we mapped N and T_g of the simulation to the experimental value as follows:

(i) First, the experimental result of the bulk T_g is fitted to the Flory−Fox equation

$$T_g(M_n) = T_{g\infty} - K/Mn \tag{8}$$

where M_n is the molecular weight, $T_{g\infty}$ is the glass transition temperature of the polymer with infinite molecular weight, and K is the material constant. The parameters $T_{g\infty}$ and K are obtained by the least-squares method as $T_{g\infty} = 379.57$ [K] and $K = 1.52 \times 10^4$ [K]. These values are not so far from those in the literature.[27]

(ii) Next, the simulation result for T_g in the bulk is also fitted by eq 8 assuming that the number of beads N and the glass transition temperature T_g^{sim} of the simulation are converted to the actual molecular weight M of PS and the actual T_g as follows:

$$M_n = \alpha N, \quad T_g = \beta T_g^{sim} \tag{9}$$

This procedure gives $\alpha = 463.8$ and $\beta = 927.74$. The mapping between N and M_n is not very much different from that of Kremer and Grest.[20] They report that the entanglement molecular weight of PS is $N = 35$ and $M_n = 18\,000$, which corresponds to $\alpha^{KG} = 514.28$. Considering that our simulation was done with the parameter r^{cut} slightly different from theirs, the agreement is reasonable.

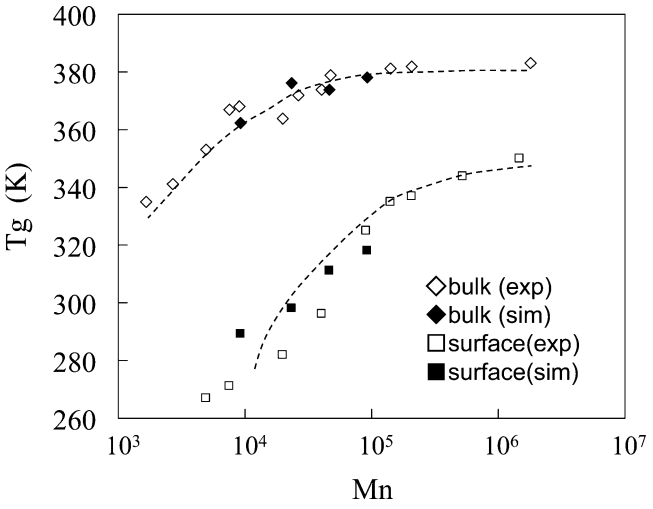

Figure 8. Glass transition temperatures are plotted against the molecular weight. Filled symbols indicate the results of MD simulation, and open symbols indicate the result of the experiment of Tanaka et al.[2]

(iii) Using same value of α and β, the simulation result T_g^{sim} of the surface is converted to actual values.

Figure 8 shows the comparison between the experimental glass transition temperature obtained by Tanaka et al.[2] and that obtained by the simulation using the above conversion. The agreement between the experiment and simulation is very good. Notice that the same conversion factors α and β are used for the bulk and the surface. This indicates that the change of the glass transition temperature near the surface is well represented by the simulation.

4. Conclusion

In this paper, we determined the glass transition temperature at the surface and in the bulk region from the temperature dependence of the mean-square displacement function of polymer segment $\phi_s(t^*;T)$ and $\phi_b(t^*;T)$. We have shown that t^* needs not be very long (t^* has been chosen to be 50τ) and that the glass transition temperature obtained by the method agrees well with that obtained by the free volume analysis. We have also shown that the method gives a good agreement with the results by scanning force microscopy.

The method proposed here does not require very long computation time and may be used to study the effect of molecular weight distribution or the effect of additives of small molecular weight, etc. We shall report these studies in the future.

Acknowledgment. The authors thank Y. Masubuchi, J. Takimoto, and T. Kawakatsu for many helpful comments and discussions. This work is supported by The Japan Science and Technology Agency (JST).

References and Notes

(1) Forrest, J. A.; Jones, R. A. L. In *Polymer Surfaces, Interfaces and Thin Films*; Karim, A., Kumar, S., Eds.; World Scientific: Singapore, 2000.
(2) Tanaka, K.; Takahara, A.; Kajiyama, T. *Macromolecules* **2000**, *33*, 7588.
(3) Kajiyama, T.; Tanaka, K.; Takahara, A. *Polymer* **1998**, *39*, 4665.
(4) Kajiyama, T.; Tanaka, K.; Satomi, N.; Takahara, A. *Sci. Technol. Adv. Mater.* **2000**, *1*, 31.
(5) (a) Keddie, J. L.; Jones, R. A.; Cory, R. A. *Europhys. Lett.* **1994**, *27*, 59. (b) Keddie, J. L.; Jones, R. A.; Cory, R. A. *Faraday Discuss.* **1994**, *8*, 219.

(6) Wallace, W. E.; Van Zanten, J. H.; Wu, W. L. *Phys. Rev. E* **1995**, *52*, R3329.
(7) Forrest, J. A.; Dalnoki-Veress, K.; Dutcher, J. R. *Phys. Rev. E* **1997**, *56*, 5705.
(8) Orts, W. J.; van Zanten, J. H.; Wu, W. L.; Satija, S. K. *Phys. Rev. Lett.* **1993**, *71*, 867.
(9) Fryer, D. S.; Nealey, P. F.; de Pablo, J. J. *Macromolecules* **2000**, *33*, 6439.
(10) Tsui, O. K. C.; Zhang, H. F. *Macromolecules* **2001**, *34*, 9139.
(11) Fukao, K.; Miyamoto, Y. *Europhys. Lett.* **1999**, *46*, 649.
(12) Kanaya, T.; Miyazaki, T.; Watanabe, H.; Nishida, K.; Yamano, H.; Tasaki, S.; Bucknall, D. B. *Polymer* **2003**, *44*, 3769.
(13) Morita, H.; Ikehara, T.; Nishi, T.; Doi, M. *Polym. J.* **2004**, *36*, 265.
(14) Torres, J. A.; Nealey, P. F.; de Pablo, J. J. *Phys. Rev. Lett.* **2000**, *85*, 3221.
(15) Varnik, F.; Baschanagel, J.; Binder, K. *Phys. Rev. E* **2002**, *65*, 021507.
(16) Aoyagi, T.; Takimoto, J.; Doi, M. *J. Chem. Phys.* **2002**, *117*, 8153.
(17) Baljon, A. R. C.; Van Weert, M. H. M.; DeGraaff, R. B.; Khare, R. *Macromolecules* **2005**, *38*, 2391.
(18) Morita, H.; Yamada, M.; Yamaguchi, T.; Doi, M. *Polym. J.* **2005**, *37*, 782.
(19) Yoshimoto, K.; Tushar, S. J.; Nealey, P. F.; de Pablo, J. J. *J. Chem. Phys.* **2005**, *122*, 144712.
(20) Kremer, K.; Grest, G. S. *J. Chem. Phys.* **1990**, *92*, 5057.
(21) Aoyagi, T.; Sawa, F.; Shoji, T.; Fukunaga, H.; Takimoto, J.; Doi, M. *Comput. Phys. Commun.* **2002**, *145*, 267.
(22) Helfand, E.; Wasserman, Z. R. *Macromolecules* **1976**, *9*, 879.
(23) Fleer, G. J.; Cohen Stuart, M. A.; Scheutjens, J. M. H. M.; Cosgrove, T.; Vincent, B. In *Polymers at Interfaces*; Chapman & Hall: London, 1993.
(24) Matsen, M. W.; Schick, M. *Phys. Rev. Lett.* **1994**, *72*, 2660.
(25) Doi M.; Edwards, S. F. *The Theory of Polymer Dynamics*; Oxford Scientific Publications: Oxford, 1986.
(26) Andersen, H. C. *J. Chem. Phys.* **1980**, *72*, 2384.
(27) O'Driscoll, K.; Sanayei, R. A. *Macromolecules* **1991**, *24*, 4479.

MA052632H